



ELSEVIER

Physica D 141 (2000) 117–132

PHYSICA D

www.elsevier.com/locate/physd

Distribution functions and excitation spectra of Toda systems at intermediate temperatures

M. Jenssen^a, W. Ebeling^{b,*}

^a *Waldkunde-Institut Eberswalde, D-16225 Eberswalde, Germany*

^b *Institute of Physics, Humboldt-University Berlin, D-10178 Berlin, Germany*

Received 9 December 1999; accepted 24 January 2000

Communicated by H. Müller-Krumbhaar

Dedicated to the 75th birthday of Youri L. Klimontovich

Abstract

The thermodynamic functions, the distribution of stochastic forces and energy, and the spectra of nonlinear excitations of 1D Toda systems embedded into a heat bath are studied. In a transition region of temperature, where the specific heat at constant length is about $\frac{3}{4}k_B T$, the systems show very specific properties that can be attributed to the interaction between solitary waves. A first one is the energy localisation at special sites in non-uniform Toda systems corresponding to multiple elastic collisions. Furthermore, we show that a finite-size Toda ring with weak thermal coupling develops in this temperature range a broadband coloured noise spectrum with an $1/f$ tail at low frequencies. © 2000 Elsevier Science B.V. All rights reserved.

Keywords: Toda systems; Distribution function; Excitation spectra

1. Introduction

Solitary waves as excitations of nonlinear chains of molecules generated considerable interest in the last 20 years [1–11]. Of special interest for the study of Toda systems is the existence of exact solutions for the dynamics and statistical thermodynamics. On this basis, it was shown in [4–9] that phonon excitations determine the spectrum at low temperatures, and strongly localised soliton excitations are the most relevant at high temperatures. In this paper we study dissipative Toda lattices including noise and friction within the intermediate temperature region where both types of excitations are present and are adequately described in terms of mutually interacting cnoidal waves. We will show here that there exists a temperature region around a transition temperature T_{tr} between the phonon and the ideal soliton regime, where the interaction of nonlinear excitations has a remarkable influence on several

* Corresponding author. Tel.: +49-2093-7636/7637; fax: +49-2093-7638.
E-mail address: ebeling@physik.hu-berlin.de (W. Ebeling)

physical phenomena, the first one being energy localisation at special sites, and another one, the excitation of a broadband coloured noise spectrum with a $1/f$ region at low frequencies. This way, we aim to contribute towards a new theory of energy activation processes as, e.g., chemical reactions in solutions or in biomolecules. Here, we will restrict ourselves to the investigation of classical Toda models of molecular systems.

In our earlier work we have shown that soft Toda springs are able to trap and superpose pulse-like excitations (solitons) impinging from the hard host lattice [11–15,31]. In thermal equilibrium, there exists a finite temperature T_{loc} where the fusion of solitons leads to a maximal localisation of potential energy at soft springs [12,13,31]. A system consisting of few soft Toda springs which are embedded into a bath of hard Toda springs might be considered as a very rough model of a dilute solution, which consists of solute molecules (possibly with active reaction sites) embedded into a bath of relatively passive molecules. In subsequent work, it was shown by MD simulations for 1D, 2D, and 3D systems of up to 200 molecules with Morse-interactions [14,15] and with finite-range Lennard-Jones potentials [16,17] as well as for the full Lennard-Jones interaction [18], that the basic effects of energy localisation persist for typical molecular forces and in higher dimensions. Energy localisation effects were studied in the spectrum of correlations [17], and the tails of the one-particle distribution function at high energies were investigated [18]. As an important result, in 1D systems, energy localisation is possible only at soft sites (springs or molecules), whereas in higher dimensions at the same temperature T_{loc} a weak localisation of potential energy takes place on hard sites also [16,17]. In this region a transition was observed from a hexagonal lattice structure for lower temperatures to a fluid-like structure of higher symmetry at temperatures right from the optimum.

In this paper, we return to the study of Toda systems in thermal equilibrium including noise and friction effects. First we will briefly revisit the most important of the older results. Then the properties of the equilibrium distribution function of the stochastic forces are investigated, in particular regarding the transition region. Energy localisation at soft sites will be shown to be a special consequence of the properties of the host system in the transition region. By numerical integration of Langevin equations we will study the time correlations of the equilibrium fluctuations of the stochastic forces. The influence of system size and varying degree of thermal coupling will be discussed.

2. Distribution functions and thermodynamic potentials of the Toda lattice

Our 1D standard model of molecular systems consists of N point masses m_i connected to the next neighbours at both sides by Toda springs. The actual distance between the mass i and the mass $i + 1$ is R_i , the equilibrium distance is assumed to be σ_i , therefore the spring elongation reads $r_i = R_i - \sigma_i$. The spring energy is described by Toda potentials

$$V(r_i; \omega_i, b_i) = \frac{m\omega_i^2}{b_i^2}(\exp(-b_i r_i) - 1 + b_i r_i), \quad (1)$$

where b_i is the stiffness of the spring i and ω_i the linear oscillation frequency around the equilibrium position. We assume then the following equations of motion:

$$\begin{aligned} \dot{r}_i &= \frac{p_{i+1}}{m_{i+1}} - \frac{p_i}{m_i}, \\ \dot{p}_i &= \left[\frac{m_{i-1}\omega_{i-1}^2}{b_{i-1}} \exp(-b_{i-1}r_{i-1}) - \frac{m_i\omega_i^2}{b_i} \exp(-b_i r_i) \right] + \gamma_i^{1/2} [(2k_B T m_i)^{1/2} \zeta_i(t) - \gamma_i^{1/2} p_i]. \end{aligned} \quad (2)$$

The second term on the r.h.s. describes noise and damping generated by a surrounding heat bath with

$$\langle \zeta_i(t) \rangle = 0, \quad \langle \zeta_i(t) \zeta_j(t') \rangle = \delta_{ij} \delta(t - t'). \quad (3)$$

The validity of an Einstein relation between noise strength and damping strength is assumed which guarantees the existence of a thermal equilibrium, independent of the friction parameter $\gamma_i \geq 0$. We note that $\gamma_i = 0$ corresponds to the conservative case.

Toda springs are exponentially hard with respect to compression and rather weak with respect to expansion. Because molecules have similar properties, we can consider the mass m_i together with the spring r_i fixed to the right side as a crude 1D model of a molecule. For simplicity let us assume in the following that all the masses $m_i = m$, all friction constants $\gamma_i = \gamma$, and all equilibrium distances $\sigma_i = \sigma$ are equal. Further we assume that in the rest state at $T = 0$ the average distance of the particles is $R_i = \sigma$, i.e., $r_i = 0$. The linear term in (1) describes the dilatation interaction and implies the artificial assumption of an infinite range potential. However, interaction is confined to the next neighbours and consequently

$$\varepsilon_i = \frac{m\omega_i^2\sigma}{b_i} \quad (4)$$

can be considered as the equivalent for the depth of the potential well in the Toda system. This quantity will be used as an energy unit in the following. We will differentiate between uniform Toda chains where all the spring parameters $b_i = b_0$ and $\omega_i = \omega_0$ are equal, and non-uniform chains where different spring parameters will occur. In this chapter we restrict our study to uniform systems and omit for simplicity all the indices.

Let us begin with the discussion of the statistical properties of a canonical ensemble of “Toda molecules” with pressure P and temperature T following the lines developed in [1,10,12]. With the abbreviations

$$X = \frac{\varepsilon}{\sigma b k_B T}, \quad Y = \frac{P}{b k_B T},$$

the distribution function of a single molecule reads

$$f(p, r) = Z_1^{-1} \exp\left(-\frac{p^2/2m + V_{\text{eff}}}{k_B T}\right),$$

$$Z_1^{-1} = \frac{bX^{X+Y}}{\sqrt{2\pi m k_B T} \exp(X)\Gamma(X+Y)} \quad (5)$$

with the effective potential

$$V_{\text{eff}}(r) = V(r) + Pr,$$

where k_B denotes the Boltzmann constant. $V(r)$ is the Toda potential according to Eq. (1). All thermodynamic functions follow by derivation of the partition function with respect to the corresponding parameters. Due to the Einstein relation the equilibrium distribution function does not depend on the friction strength γ .

The mean specific volume is given by

$$v = \frac{1}{b}(\ln X - \Psi(X+Y)) + \sigma. \quad (6)$$

From this the pressure P is determined by

$$P = b k_B T \Psi^{-1}[\ln X - b(v - \sigma)] - \frac{\varepsilon}{\sigma}, \quad (7)$$

where the digamma-function Ψ is defined as usual by the logarithmic derivative of the Γ -function.

The specific internal energy of the system is given by

$$e = \frac{E}{N} = \frac{1}{2}k_B T + \langle u \rangle. \quad (8)$$

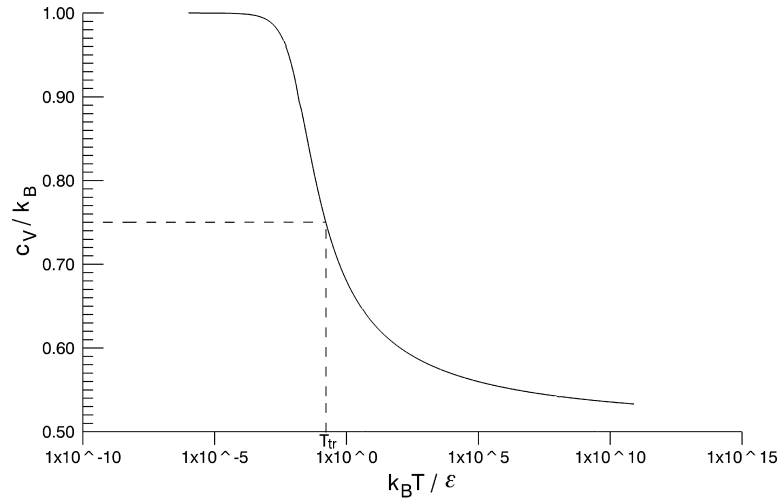


Fig. 1. Specific heat per molecule c_V at constant length of the Toda chain. In the region around the transition temperature T_{tr} (defined by $c_V(T_{tr}) = \frac{3}{4}k_B$) we observe the most interesting physical effects due to the interaction between solitary waves. For the chosen parameters $v = \sigma$ and $b = 100/\sigma$, we obtain $T_{tr}k_B = 0.16\varepsilon$.

The mean potential energies read

$$\langle u \rangle = \frac{P}{b} + \frac{\varepsilon}{b\sigma} (\ln X - \Psi(X + Y)), \quad (9)$$

where the pressure P is given by Eq. (7). At low temperatures the equipartition theorem holds and we find

$$\langle u \rangle = \frac{1}{2}k_B T. \quad (10)$$

In the high-temperature limit, the ‘‘Toda molecules’’ behave like hard spheres and the potential energies disappear.

The specific heat per molecule at constant volume reads [10]

$$c_V = k_B \left(\frac{1}{2} + X + Y - \frac{1}{\Psi'(X + Y)} \right), \quad (11)$$

where the trigamma-function Ψ' is defined as usual by the second logarithmic derivative of the Γ -function. This function tends to k_B in the low-temperature regime due to the thermal energy $k_B T$ of each phonon. On the other hand, c_V shows the properties of a 1D hard-sphere gas at high temperatures, i.e., c_V tends to $\frac{1}{2}k_B$.

As was shown in [6], for constant total length, all the thermodynamic functions can be obtained from the phenomenology of an ideal soliton gas in the high-temperature limit, each soliton possessing a mean thermal energy of $\frac{1}{2}k_B T$. Several papers were devoted to the reconstruction of thermal properties of Toda systems from a phonon–soliton phenomenology for intermediate temperatures beyond the ideal phonon gas and the ideal soliton gas [4–9]. For low temperatures the number of thermal solitons increases with $T^{1/3}$, but it tends to the number of molecules at high temperatures [7–9,30]. Here we introduce a transition temperature T_{tr} corresponding to $c_V = \frac{3}{4}k_B$ (Fig. 1), where deviations from the low-temperature behaviour of the soliton density become significant. In the region around T_{tr} , thermal excitations should be described more generally as cnoidal waves which contain both phonons and solitons as special cases in the low- and high-amplitude limit, respectively [1]. Loosely speaking, cnoidal or solitary waves can be considered as deformed phonons with more or less steep compression humps and shallow dilatation valleys between them. In the transition region, the interaction between solitary-wave excitations may lead to interesting physical effects as will be demonstrated in the following sections.

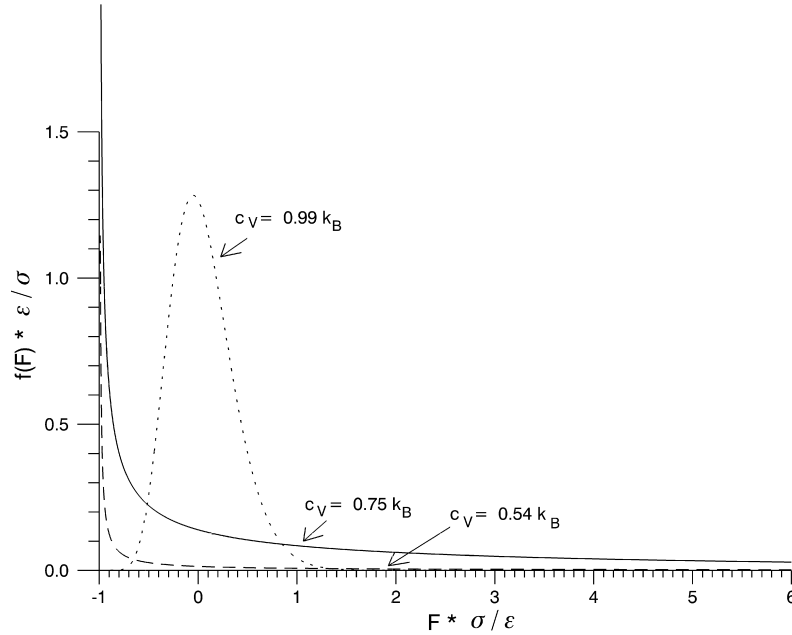


Fig. 2. Distribution function of the force F in an infinite Toda chain with constant length, $v = \sigma$, and $b = 100/\sigma$ (Eqs. (7) and (13)). The function is plotted for three different temperatures corresponding to the phonon regime (dotted), the transition region (solid), and the hard-core regime dominated by strongly localised solitons (dashed).

In the remainder of this section we will discuss the time-independent properties of the stochastic forces. According to (1) the force F acting on a molecule is given by

$$F = \frac{\varepsilon}{\sigma} (\exp(-br) - 1). \quad (12)$$

The equilibrium distribution is derived from Eqs. (5) and (12) yielding

$$f(F) = \frac{\sigma}{\varepsilon} \frac{X^{X+Y}}{\exp(X)\Gamma(X+Y)} \left(1 + \frac{\sigma F}{\varepsilon}\right)^{X+Y-1} \exp\left(-\frac{\sigma X F}{\varepsilon}\right). \quad (13)$$

In the low-temperature limit, we find the well-known symmetrical shape of the distribution function around the mean value $F = 0$, which is obtained for harmonic lattices (Fig. 2). With increasing temperature, the distribution becomes biased and the maximum is shifted towards the left. As can be seen from Eq. (13) for $X + Y < 1$, the probability density diverges at $F = -\varepsilon/\sigma$, whereas the integral over the F -axis yields 1. According to Eq. (12) the value $F = -\varepsilon/\sigma$ corresponds to an infinite dilatation r . This behaviour reflects the tendency of the molecules of the chain to drift apart as a result of collisions, i.e., due to the presence of thermal solitons. As can be obtained from Eq. (11), this behaviour is observed for $c_V < 0.89k_B$, i.e., both in the transition region and in the region of non-interacting solitons. In the latter case, if T tends to infinity, the distribution function tends to get a rectangular shape consisting of a narrow peak at $F = -\varepsilon/\sigma$ and a shallow but long-range tail for large F values which is typical for hard collisions (Fig. 2). In contrast, at the transition temperature, we observe a relatively broad distribution with an exponential decay for large F . This behaviour reflects the dominance of “soft” collisions with relatively long interaction range.

By integration we find the mean value of the force F

$$\langle F \rangle = P, \quad (14)$$

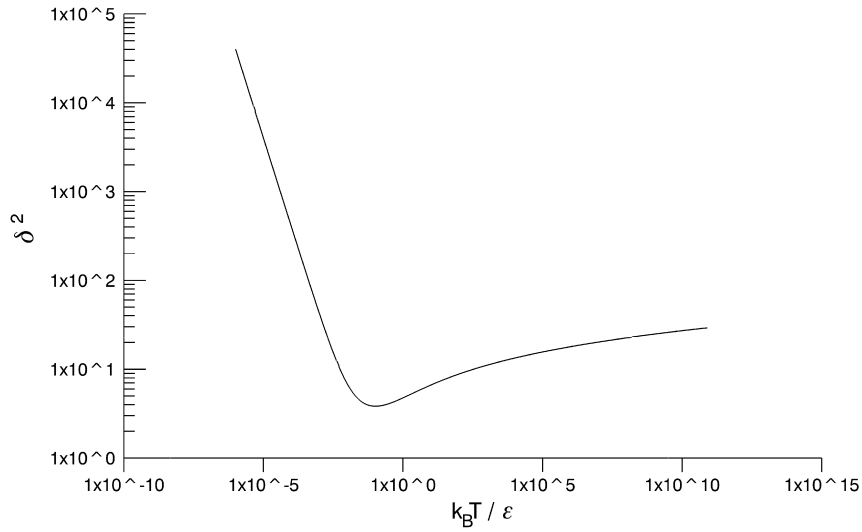


Fig. 3. Relative mean square fluctuation (Eq. (15)) of the random force acting on a Toda molecule in a chain with fixed total length (Figs. 1 and 2) with dependence on the temperature. The minimum occurs near to the transition temperature T_{tr} .

and the relative mean square deviation reads

$$\delta^2 = \frac{\langle \delta F^2 \rangle}{\langle F \rangle^2} = \left(\frac{m\omega^2}{P^2} + \frac{b}{P} \right) k_B T. \quad (15)$$

Representing this quantity as a function of temperature, we see that the relative mean square deviation has a minimum near to the transition temperature T_{tr} (Fig. 3).

Finally, we notice that in the case of fixed total length the distribution functions (Eqs. (5) and (13)) are exactly valid only in the thermodynamic limit, i.e., for an infinite number of molecules. This is due to the fact that we fixed the volume only in the thermal average by Eq. (6). Hence the nature of fluctuations around the mean values may be modified for decreasing number of molecules in the chain. In particular, in a finite Toda chain, the probability density of the force F cannot diverge at $F = -\varepsilon/\sigma$. With the constraint of periodic boundary conditions, the expansion tendency of a finite Toda ring around T_{tr} may lead to a strong coherence of the molecular motion affecting the time correlations of the fluctuations, as will be shown in Section 4.

3. Solutions of soft molecules in a hard Toda chain

Now we will extend our model to the case of dilute solutions of n chemical sorts, each represented by N_s soft ‘‘Toda molecules’’ with stiffness b_s ($s = 1, \dots, n$) in a bath of N_0 hard ‘‘Toda molecules’’ ($b_s < b_0$) at constant volume. In the limit $b_0 \rightarrow \infty$, the bath becomes a 1D hard-core gas. In the following we assume $N_s \ll N_0$. Then the pressure is determined by the bath of hard molecules and remains the same as before (Eq. (7)). The internal energy of the system is given by

$$E = \frac{1}{2} k_B T \left(N_0 + \sum_s N_s \right) + N \langle u_0 \rangle + \sum_s N_s \langle u_s \rangle. \quad (16)$$

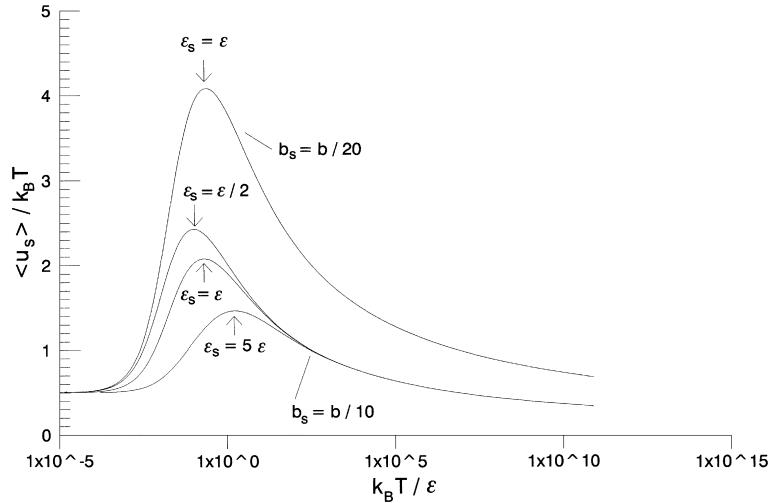


Fig. 4. In the transition region around T_{lr} the mean potential energy of soft “Toda molecules” diluted in a hard Toda chain at fixed total length (parameters as in Figs. 1–3) shows a pronounced maximum. The potential energy of the soft molecules increases linearly with the inverse of their stiffness parameter b_s . With decreasing binding energy ϵ_s , the relative maximum is shifted to lower temperatures (lower three curves).

The mean potential energies of hard and soft molecules, respectively, read [12]

$$\langle u_0 \rangle = \frac{P}{b_0} + \epsilon_0 \left(\frac{v}{\sigma} - 1 \right), \quad (17)$$

$$\langle u_s \rangle = \frac{P}{b_s} + \frac{\epsilon_s}{b_s \sigma} (\ln X_s - \Psi(X_s + Y_s)), \quad (18)$$

where the pressure P is given by Eq. (7). At low temperatures the equipartition theorem holds and we find

$$\langle u_0 \rangle = \langle u_s \rangle = \frac{1}{2} k_B T. \quad (19)$$

In the high-temperature limit, the ‘Toda molecules’ behave like hard spheres and the potential energies disappear. Especially, we find from Eqs. (7), (17) and (18) for the case $v = \sigma$

$$\langle u_s \rangle = \frac{b_0}{b_s} \langle u_0 \rangle. \quad (20)$$

In previous work, this exact result was reconstructed from a gas of non-interacting solitons which dominate the dynamics at high temperatures [12]. It was also shown that at intermediate temperature, the mean potential energy of soft molecules reaches a maximum in units of thermal energy $k_B T$ (Fig. 4). This effect was explained by the superposition of thermal excitations at the soft molecules corresponding to multiple elastic collisions.

Now we will study this maximum in more detail. From the localisation condition

$$\frac{d(\langle u_s \rangle / T)}{dT} = 0, \quad (21)$$

we find using Eqs. (7) and (18)

$$\ln X_s - \Psi(X_s + Y_s) - \frac{b_0 \Psi'(X_s + Y_s)}{b_s \Psi'(X_0 + Y_0)} + \frac{\epsilon}{\epsilon_s \Psi'(X_0 + Y_0)} + \frac{(\epsilon_s - \epsilon)}{\epsilon_s} (1 - X_s \Psi'(X_s + Y_s)) = 0. \quad (22)$$

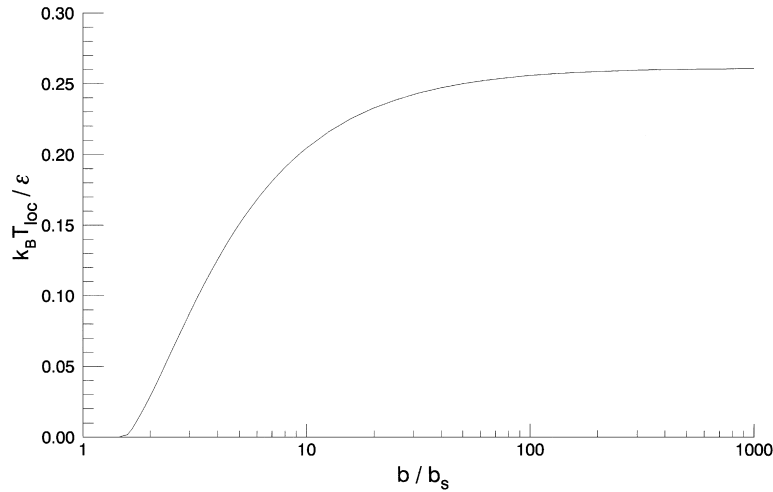


Fig. 5. Temperature T_{loc} of the maximum energy localisation of soft “Toda molecules” (Fig. 4) as a function of their stiffness parameter b_s for $\varepsilon_s = \varepsilon$. For a sufficient low stiffness of the diluted molecules the localisation temperature depends on the properties of the hard Toda bath only. For the chosen parameters the value $T_{\text{loc}} = 0.26\varepsilon$ corresponds to a specific heat $c_V(T_{\text{loc}}) = 0.73k_B$ indicating the transition region.

Eq. (22) can be solved together with (7) numerically yielding the temperature T_{loc} defining the maximum localisation point. According to Eq. (4), ε_s can be interpreted as the depth of the potential well or binding energy of the soft molecules. For a given stiffness b_s , it defines the linear oscillation frequency of the soft molecules. With decreasing ε_s the localisation point T_{loc} is shifted to lower temperatures, but $\langle u_s(T_{\text{loc}}) \rangle / k_B T_{\text{loc}}$ increases slightly (cf. curves in Fig. 4). This means that mainly low-amplitude or phonon-like excitations will be localised at the soft sites with decreasing linear oscillation frequency. However, the time-scale for high-amplitude or soliton-like excitations is given by the stiffness parameter. Hence the amount of collimated energy $\langle u_s(T_{\text{loc}}) \rangle / k_B T_{\text{loc}}$ increases significantly with decreasing b_s (cf. upper curve in Fig. 4) due to the enhanced superposition of thermal solitons [11,12].

In order to study this effect in more detail we will set $\varepsilon_s = \varepsilon$ in the following. For sufficiently low stiffness b_s of the diluted molecules, the localisation temperature T_{loc} depends on the properties of the surrounding hard Toda chain only (Fig. 5). This behaviour was already observed in molecular-dynamics simulations of more realistic 3D models of dense fluids [16].

In particular, for a vanishing ratio of stiffness parameters b_s/b_0 , the localisation condition (22) can be simplified, yielding

$$\ln X_0 - \ln(X_0 + Y_0) + \frac{1}{\Psi'(X_0 + Y_0)} \left(\frac{1}{X_0} - \frac{1}{X_0 + Y_0} \right) = 0. \quad (23)$$

Solving this equation together with Eq. (7) and inserting the solution into Eq. (11) we obtain for the specific heat at the localisation point

$$c_V(T_{\text{loc}}) \simeq 0.73, \quad (24)$$

yielding a good agreement with the definition of the transition temperature T_{tr} given above. This result confirms the statement that energy localisation at soft sites is a special consequence of solitary-wave interaction in the transition region.

Finally we obtain from Eqs. (17), (18) and (23) for the mean potential energy of soft molecules at localisation temperature a linear relation to the ratio of stiffness parameters

$$\langle u_s(T_{\text{loc}}) \rangle = \text{const.} \frac{b_0}{b_s} k_B T_{\text{loc}}. \quad (25)$$

Energy localisation at soft sites in thermal equilibrium is due to the pressure P produced by the bath of hard molecules in the transition region and can be attributed to the superposition of solitary waves corresponding to multiple elastic collisions. According to Eq. (14), the pressure P acts as a random force with a non-zero mean on the soft molecules. Hence the distribution functions (5) of the soft molecules are raised up to higher energies. If we interpret the soft molecule as a reactive site with a certain activation barrier, this force P may lead to a considerable enhancement of the transition rate in the region of T_{loc} as was shown within the frame of elementary transition-state theory [12–15,31].

4. Time correlations: transformation of white into coloured noise with $1/f$ tail

Besides the static localisation effect discussed in Section 3 we expect novel effects concerning the nature of fluctuations around the equilibrium functions due to the interaction of nonlinear excitations in the transition region. So, we will now proceed to the investigation of time correlation functions (ACF) and the derived spectra. In this section we restrict ourselves to the investigation of uniform Toda systems. Since the analytical theory of the ACF is restricted to the harmonic case, we rely on computer experiments in the following. Correlation functions from molecular-dynamic simulations of Toda systems were calculated, e.g., in [4,5], mainly in order to identify thermally activated solitons in the spectra. Here, we ask the question if Toda systems may transform the uncorrelated fluctuations of the surrounding heat bath, which are modelled by the Gaussian white noise $\zeta(t)$ in Eq. (3), into some kind of coloured noise that may favour low-frequency activation processes. This question is of central importance, especially for the understanding of transition processes in complex biomolecules [14,19–24,32].

In contrast to the equilibrium properties following from the distribution function (5), the time correlation functions depend on the friction parameter γ , because its inverse determines the characteristic relaxation time of the system (2). In the conservative case $\gamma = 0$, the system follows the Hamiltonian dynamics. With increasing γ , the Hamiltonian dynamics is modified, and for large γ the “Toda molecules” reproduce the white noise of the surrounding heat bath. So, we performed our simulations of the Langevin equations (2) and (3) for the case of weak thermal coupling with $\gamma = 10^{-3}\omega_0$. For integration we used a Runge–Kutta algorithm of fourth order using a constant stepsize of $10^{-3}/\omega_0$ including white-noise sources according to Eq. (3). First the system was heated up to a temperature around T_{tr} . After attaining the thermal equilibrium, we calculated the one-particle ACF of the forces (12) from the trajectory

$$\text{ACF}(t) = \langle \delta F(t_0 + t) \delta F(t_0) \rangle_{t_0}. \quad (26)$$

From this we calculated the spectrum $(\text{FF})_\omega$ defined as the Fourier transform of Eq. (26).

For low temperatures the Toda system behaves like a harmonic lattice and the dynamics is determined by the phonons. Fig. 6 shows the force spectrum calculated from a long-term simulation of a molecular ring consisting of $N = 10$ identical “harmonic molecules” subject to periodic boundary conditions. As expected, the excitation spectrum shows five distinct peaks at the well-known normal-mode frequencies. Naturally, the white noise of the surrounding heat bath is reproduced at low frequencies. For $N \rightarrow \infty$ the thermal energy will be distributed equally among an infinite number of phonons, the distinct peaks disappear and we observe a white-noise spectrum over the entire frequency range. On the other hand, for high temperatures, the Toda spectrum behaves like an ideal hard-core gas characterised by the simple white noise again.

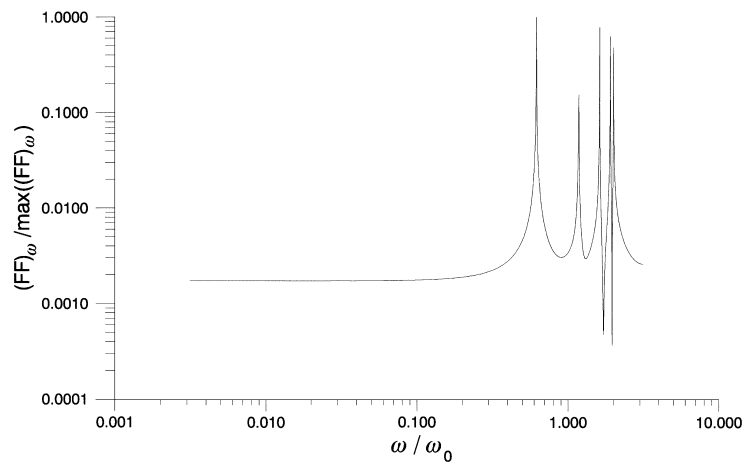


Fig. 6. Spectra $(FF)_\omega$ of single-particle forces F in a uniform ring of $N = 10$ harmonic oscillators with oscillation frequency ω_0 in thermal equilibrium with a heat bath in the transition-temperature region. The friction parameter is $\gamma = 10^{-3}\omega_0$. The spectrum was obtained by Fourier transformation of the ACF at the sampling interval $1/\omega_0$ calculated from a trajectory integrated over the time $10\,000/\omega_0$. We observe the phonon peaks at $\omega/\omega_0 = 2 \sin(i\pi/10)$ ($i = 1, \dots, 5$) as well as a white-noise tail at low frequencies.

However, Fig. 7 shows the excitation spectra of the one-particle ACF (26) obtained from a simulation of a uniform Toda ring (2) made up of $N = 10$ and of $N = 20$ “Toda molecules” in the transition-temperature region. Most strikingly, in the double-logarithmic presentation we observe a straight line with a slope near to -1 clearly indicating a broadband coloured noise of $1/f$ type at low frequencies. The trajectory of the molecular force F shows that the high-energy events corresponding to high-compression peaks or solitary waves occur most likely in clumps as it is typical for beating phenomena (Fig. 8). In particular, the $1/f$ spectrum implies a hierarchy of beatings where

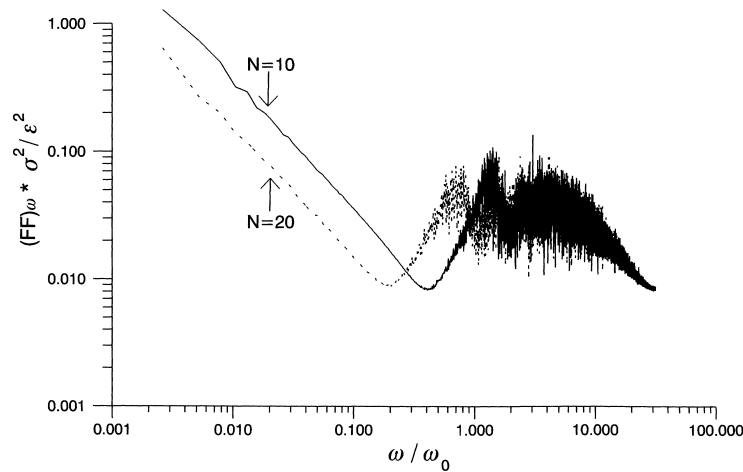


Fig. 7. Spectra $(FF)_\omega$ of single-particle forces F in uniform rings of $N = 10$ (solid) and $N = 20$ (dashed) Toda oscillators with oscillation frequency ω_0 and stiffness $b = 100/\sigma$ in thermal equilibrium with a heat bath in the transition-temperature region ($k_B T = 0.26\epsilon$ corresponds to $c_V(T_{loc}) = 0.73k_B$). The friction parameter is $\gamma = 10^{-3}\omega_0$. The spectra were obtained by Fourier transformation of the ACF (Fig. 11) at a sampling interval of $0.1/\omega_0$ calculated from a trajectory of the length $30\,000/\omega_0$. We observe broad peaks around the second-phonon frequencies as well as $1/f$ tails at the low end of the spectra. The intensity decreases with particle number N .

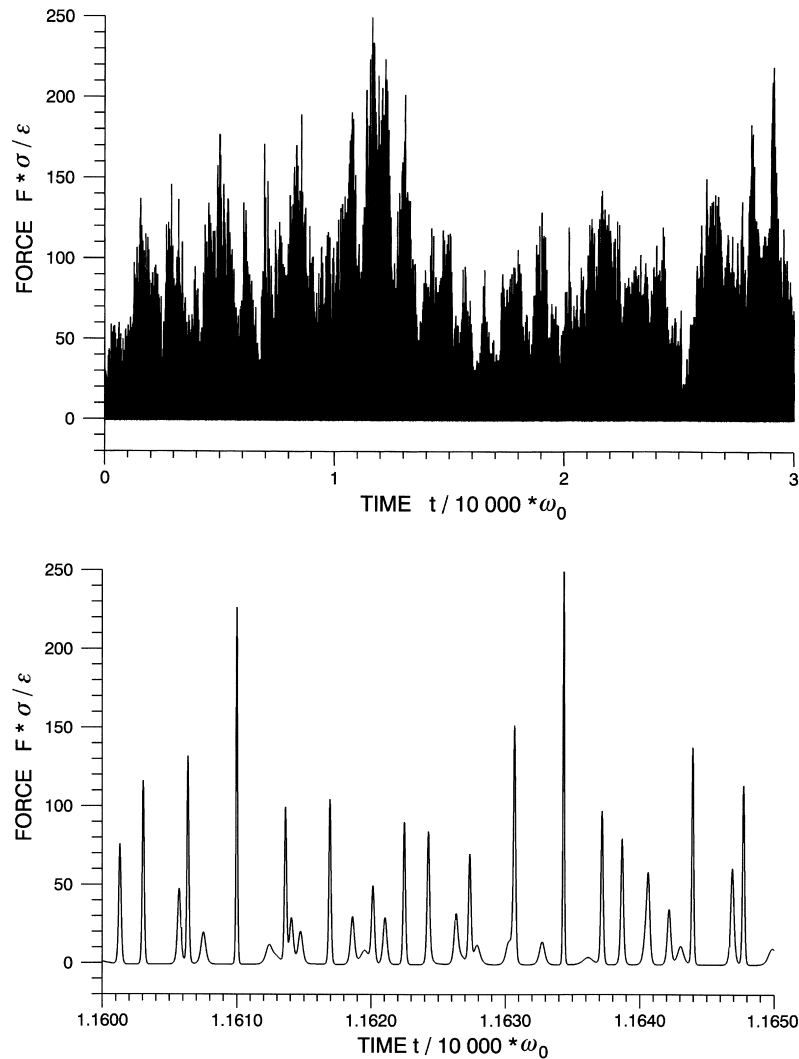


Fig. 8. Trajectory of the force F acting on a “Toda molecule” embedded in the 10-particle Toda ring in the transition region corresponding to the spectrum shown in Fig. 7. The long-term trajectory shown above indicates the hierarchy of long-range fluctuations as it is typical for $1/f$ noise. The maximum bump of the above simulation is plotted in higher resolution. We observe the beating-like modulation of the amplitudes of solitary-wave peaks.

periods with more energetic compression pulses are more probable to appear at longer time intervals. The internal dynamics is accompanied by long-term correlated random rotations of the whole ring (Fig. 9). These coherent fluctuations of the ring correspond to a diffusion regime. With respect to the spectrum of fluctuations, there is some analogy to the traffic-jam models which are classical examples of $1/f$ noise [25,26]. In this analogy the “Toda molecules” correspond to “cars” moving around a circular highway and the compression peaks make up the jams of different size. However, our “Toda molecules” do not possess a “fuel tank” and are driven only by the Brownian motion of the surrounding heat bath. Consequently, the long-term average of the velocities tends to zero. We stress that the Toda ring is in thermal equilibrium and the $1/f$ tail of the spectrum reflects the character of equilibrium fluctuations.

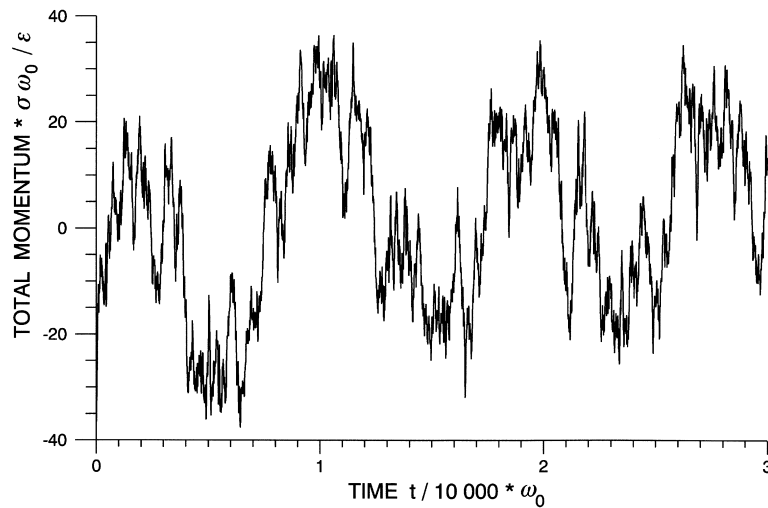


Fig. 9. Total momentum $\sum_{i=1,10} p_i$ of the 10-particle Toda ring corresponding to the simulation shown in Figs. 7 and 8. The ring rotates as a whole at low frequencies.

The hierarchical order of the fluctuations is due to the Hamiltonian dynamics of the finite-size Toda ring. Finally, let us try to get a hint on this underlying dynamics by comparison of the spectra of the harmonic and the Toda ring in more detail (Fig. 10). We notice the complete failure of the first phonon peak in the Toda spectrum. In the harmonic ring, this excitation corresponds to a standing wave with two knots which can be decomposed into two waves of the same frequency but running in opposite directions. Indeed, on the Toda ring we observe during the

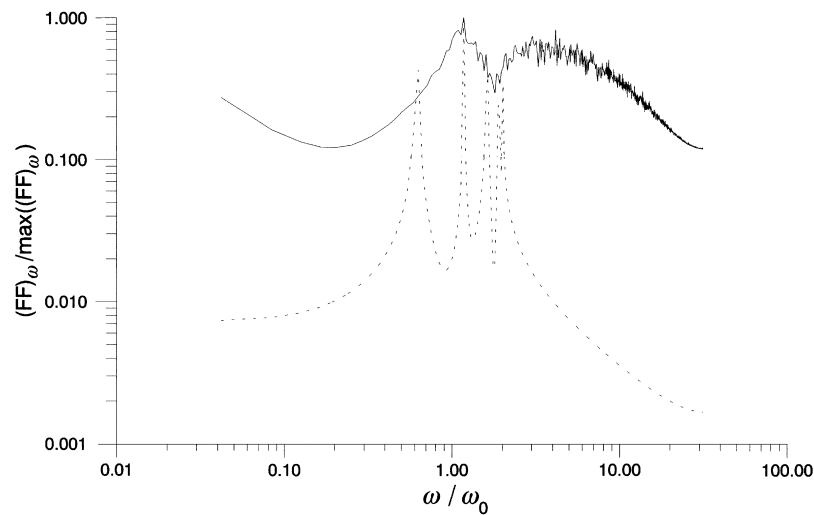


Fig. 10. Comparison of the spectra $(FF)_\omega$ of a 10-particle Toda ring (solid line) and a harmonic ring (dotted line) in thermal equilibrium with a heat bath in the transition-temperature region in the range of normal-mode frequencies. Parameters as in Figs. 7 and 8. The spectra were obtained by a Fourier transformation of the ACF at the sampling interval $0.1/\omega_0$ calculated from trajectories over the time $7000/\omega_0$. We observe the complete failure of the first-phonon peak, a broad peak around the second-phonon frequency, and a high-frequency bump right from the phonon-range in the Toda spectrum.

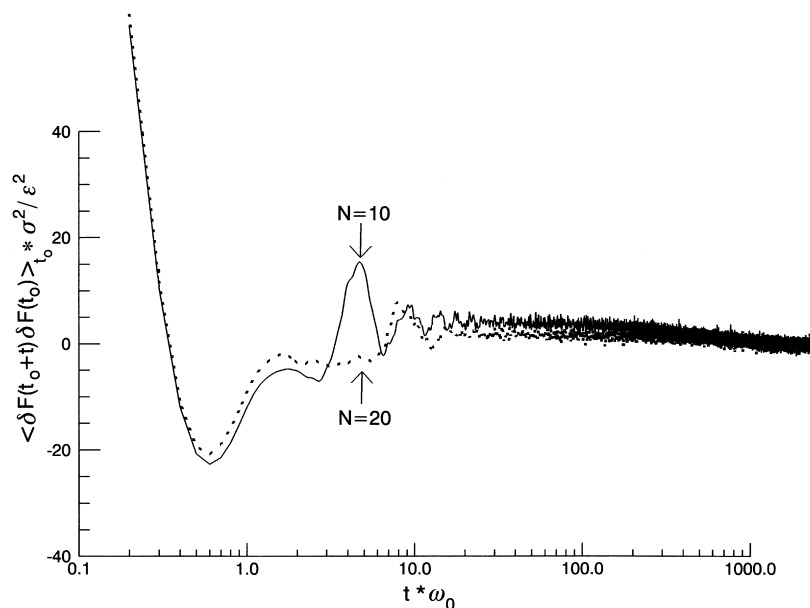


Fig. 11. Autocorrelation functions ACF(t) of the random force F for 10-particle (solid) and 20-particle (dashed) Toda rings corresponding to the spectra shown in Fig. 7. In the 10-particle ring we observe a distinct peak corresponding to two solitary waves running in opposite directions. In the 20-particle ring the corresponding peak is shifted to the right but less pronounced.

simulations, mostly two distinct soliton-like wave peaks running in opposite directions and merging into mainly one wave peak twice in each turn (Fig. 8b). The frequency of these solitary waves corresponds to the broad peak in Figs. 7 and 10 which has its maximum accurately at the second-phonon frequency. Furthermore, the speed of the nonlinear waves is varied with the fluctuations of their amplitudes and hence we do not have a fixed phase relation leading to standing-wave phenomena. Instead, we observe a beating-like modulation of the amplitude of compression peaks due to the strong interaction of mainly two solitary or cnoidal waves each of wavelength N and a frequency fluctuating around that of the second harmonic normal mode.

From the simulations, presented we not only observe a dependence of the effect on the temperature and the degree of thermal coupling, but we also presume a great importance of the boundary conditions and hence a dependence on the size of the Toda ring. The coherence of the molecular motion gets lost with increasing number of molecules. It follows from the ACF presented in Fig. 11 that the distinct solitary-wave peak corresponding to the second-phonon frequency will not only shift to the right on the time axis but also gets less pronounced with increasing N . The thermal energy gets more equally distributed over a broad spectrum of cnoidal waves with varying wavelength and frequencies instead of being contained in mainly two strongly interacting pulses. Hence the solitary-wave peak at the second-phonon frequency decreases with increasing N in the spectra of the ACF (Fig. 7). Accordingly, both the onset frequency and the intensity of the $1/f$ noise at the low end of the spectrum decrease with increasing number of molecules (Fig. 7). We conclude from these observations that the $1/f$ noise at the low end of the spectrum is a typical finite-size effect disappearing in the thermodynamic limit [19].

5. Discussion and conclusions

The investigation of distribution functions and excitation spectra in classical models of molecular systems is of central importance to the further development of the theory of molecular activation processes. After the

pioneering works of Arrhenius, in 1940 Kramer succeeded in establishing a stochastic theory of reaction rates concerning simple chemical reactions in solutions. According to the Kramers theory (for a survey we refer to [27]), reactions proceed due to transitions over an energy barrier caused by microscopic thermal fluctuations of the heat bath. The need for further generalisation of this quite successful theory originates from the fact that several activation phenomena in complex molecular systems as, e.g., enzymatic reactions or protein-folding processes, remain unexplained so far. Up to now a lot of work has been done in order to extend the original Kramers theory to more complicated reactions and to treat the coupling of non-reactive molecular systems to the reactive site explicitly.

As simple 1D models of excitations in molecular systems, we investigated here Toda systems which admit exact solutions for the dynamics and statistical thermodynamics. In the transition-temperature region, the strong interaction between solitary waves may lead to a considerable enhancement of transition rates via two different mechanisms. The first one is the energy localisation at “soft” reaction sites embedded in a hard Toda chain of fixed total length. In previous papers [12–15,31], we estimated reaction rates according to transition-state theory assuming equilibrium distributions of coupled reaction systems yielding considerable rate enhancements at intermediate temperatures. This enhancement follows from the non-zero average force (pressure) which acts on a soft reactive molecule and is of static character. This force affects the exponential factor of the rate constant significantly by lowering the activation barrier. The effect can be interpreted as a superposition of solitary waves which becomes possible at “soft” molecules at intermediate temperatures. It is not restricted to 1D Toda lattices but persists also in more realistic 2D and 3D models of dense fluids consisting of solvent and solute molecules with Morse or Lennard–Jones interactions. Superposition of solitons corresponds to multiple collisions in these systems. In higher dimensions a weak localisation of potential energy was observed also at the bindings of the bath molecules and was connected to a transition between different lattice configurations [16,17].

Besides this static effect, a considerable rate enhancement can be expected from a transformation of the uncorrelated noise of a surrounding heat bath into a broadband coloured noise with an $1/f$ tail at low frequencies. This behaviour was proven for a finite-size Toda ring with weak thermal coupling in the transition-temperature range. Such a system seems to be an ideal host for the excitation of special active sites possessing resonance frequencies inside this low-frequency band. The finite-size Toda ring with moderate coupling to a surrounding heat bath in the transition-temperature region is perhaps the simplest classical model of a ring-shaped biomolecule in solution. In previous papers real molecular forces in proteins and DNA were fitted to Toda and Morse potentials yielding the important result that the transition-temperature region corresponds to the range of physiological temperatures [12–15,30,31]. Indeed, statistical analyses of experimentally observed single-molecule trajectories of the enzyme cholesterol oxidase revealed significant and slow fluctuations in the reaction rate [24]. This effect was described as a molecular memory phenomenon, in which an enzymatic turnover is not independent of its previous turnovers because of slow fluctuations of protein conformation. Such long-term correlated conformational changes which are relevant in context with protein-folding processes and enzyme reactions might be explained by dynamical mechanisms similar to those observed in our simple Toda model. Here we found coherent molecular motions, in particular mainly two soliton-like waves of similar amplitude and frequency running in opposite directions. The fluctuations of their amplitudes and frequencies lead to some kind of nonlinear beating phenomenon that is connected to a $1/f$ region of the spectrum.

The two main types of $1/f$ -noise systems discussed so far in the literature are:

1. flicker noise observed in simple physical systems [28],
2. long-correlated noise observed in complex systems in nature and society [29].

As shown by Klimontovich, flicker noise may be interpreted as a diffusion regime of the dynamics of finite systems. Typical properties of the flicker noise of Klimontovich-type are the following:

1. This type of flicker noise appears at frequencies ω_{fl} bounded from above by the diffusion time L^2/D and from below by the observation time t_{obs}

$$\left(\frac{1}{t_{\text{obs}}}\right) < \omega_{\text{fl}} < \left(\frac{D}{L^2}\right), \quad (27)$$

where D is the diffusion constant (corresponding here to the rotational stochastic motion shown in Fig. 9) and L the length of the system (corresponding here to $N\sigma$).

2. The amplitude of the flicker noise is proportional to $1/(N\omega)$, where N is the particle number.

A quite different type of $1/f$ noise has been observed in large and complex many-particle systems far away from thermal equilibrium. The latter type of $1/f$ noise is of central importance in the theory of self-organised criticality [29].

In this paper, we presented a relatively simple dynamical system fluctuating in thermal equilibrium that transforms the uncorrelated, white noise of the surroundings into noise of $1/f$ -like type. In many respects the noise we have observed corresponds to a flicker noise of the type investigated by Klimontovich since it is clearly connected with a diffusion type of dynamics as shown in Fig. 9 and since it seems to decrease with a dependence $1/N$. A closer inspection of this point however, requires more extensive simulations; therefore we have to leave this question to further investigations. Even at the present stage of the investigations we may draw some general conclusions.

The $1/f$ noise observed in Toda systems is not connected to a fine-tuning of temperature, structural parameters, particle number, or thermal coupling, but occurs in a wide range of these quantities with varying intensity. Furthermore, it can be expected to persist for a wide class of more realistic molecular potentials in the transition region. However, it was not observed in previous investigations for Lennard–Jones molecules at higher dimensions so far [16]. This point needs further clarification and we propose to repeat the runs presented in [16] with higher accuracy, in particular extending the length of the trajectories. From the investigations carried out so far we hypothetically derive the following preconditions for fluctuating equilibrium systems to transform white noise into $1/f$ -like noise:

1. Nonlinear, asymmetrical interactions between molecular units with a steep repulsive and a flat attractive branch.
2. Quasi-1D configurations of a finite many-body system with periodic boundary conditions (ring).
3. Weak thermal coupling to a surrounding heat bath in the transition-temperature region.

We hope that the further investigation of the effects shown in this paper will support the understanding of complex molecular motions and energy activation processes. In particular, we consider a molecular ring in the diffusion regime as an ideal host for the excitation of special active sites possessing resonance frequencies inside this low-frequency band. A possible field of applications is the dynamics of chemical reactions [15,20,26] and in particular of biomolecules with enzymatic activity [21–24,32].

Acknowledgements

The authors are grateful to G. Hofmann (Eberswalde), Yu.L. Klimontovich (Moscow), Yu.M. Romanovsky (Moscow) and M. Velarde (Madrid) for support and discussions, and to a referee for useful comments on a previous version of this paper.

References

- [1] M. Toda, *Nonlinear Waves and Solitons*, Kluwer Academic Publishers, Dordrecht, 1983.
- [2] J.A. Krumhansl, J.R. Schrieffer, *Phys. Rev. B* 11 (1975) 3535.
- [3] H. Büttner, F.G. Mertens, *Solid State Commun.* 29 (1979) 663.

- [4] T. Schneider, E. Stoll, *Phys. Rev. Lett.* 45 (1980) 997.
- [5] S. Diederich, *Phys. Rev. B* 24 (1981) 3186.
- [6] H. Bolterauer, M. Opper, *Z. Phys. B* 42 (1981) 155.
- [7] F. Yoshida, T. Sakuma, *Phys. Rev. A* 25 (1982) 2750.
- [8] M. Opper, *Phys. Lett. A* 112 (1985) 201.
- [9] N. Theodorakopoulos, N.C. Bacalis, *Phys. Rev. B* 46 (1992) 10706.
- [10] M. Toda, N. Saitoh, *J. Phys. Soc. Jpn.* 52 (1983) 3703.
- [11] W. Ebeling, M. Janssen, *Physica D* 32 (1988) 183.
- [12] M. Janssen, *Phys. Lett. A* 159 (1991) 6.
- [13] W. Ebeling, M. Janssen, *Ber. Bunsenges. Phys. Chem.* 95 (1991) 1356.
- [14] W. Ebeling, M. Janssen, Yu.M. Romanovskii, in: W. Ebeling, H. Ulbricht (Eds.), *Irreversible Processes and Selforganization*, Teubner (BSB), Leipzig, 1989.
- [15] M. Janssen, W. Ebeling, in: J. Popielawski, J. Gorecki (Eds.), *Far-from-equilibrium Dynamics of Chemical Systems*, World Scientific, Singapore, 1991.
- [16] W. Ebeling, V.J. Podlipchuk, *Z. Phys. Chem.* 193 (1996) 207.
- [17] W. Ebeling, A.A. Valuev, V.J. Podlipchuk, *J. Mol. Liquids* 73/74 (1997) 445.
- [18] W. Ebeling, M. Sapeshinsky, A. Valuev, *Int. J. Bifurcat. Chaos* 8 (1998) 755.
- [19] W. Ebeling, M. Janssen, in: *Proceedings of the International Conference on Nonlinear Optics, Saratov, 1998*, SPIE 3726 (1999) 112.
- [20] R. Regeida, A. Romero, A. Sarmiento, K. Lindenberg, *J. Chem. Phys.* 111 (1999) 1373.
- [21] G.R. Welch, B. Samogyi, S. Damjanovich, *Prog. Biophys. Mol. Biol.* 39 (1982) 109.
- [22] B. Havsteen, *J. Theoret. Biol.* 140 (1989) 101.
- [23] A.Yu. Chikishev, N.V. Netrebko, Yu.M. Romanovsky, W. Ebeling, L. Schimansky-Geier, A.V. Netrebko, *Int. J. Bifurcat. Chaos* 8 (1998) 921.
- [24] H.P. Lu, L. Xun, X.S. Xie, *Science* 282 (1998) 1877.
- [25] K. Nagel, M. Paczuski, *Phys. Rev. E* 51 (1995) 2909.
- [26] D. Helbing, *Verkehrsdynamik*, Springer, Berlin, 1997.
- [27] P. Hänggi, P. Talkner, M. Borkovec, *Rev. Mod. Phys.* 62 (1990) 251.
- [28] Yu.L. Klimontovich, *Statistical Theory of Open Systems*, Kluwer Academic Publishers, Dordrecht, 1995.
- [29] P. Bak, *How Nature Works*, Springer, New York, 1996.
- [30] V. Muto, A.C. Scott, P.L. Christiansen, *Phys. Lett. A* 136 (1989) 33.
- [31] W. Ebeling, M. Janssen, *Physica A* 188 (1992) 350.
- [32] B. Havsteen, *J. Theoret. Biol.* 151 (1991) 557.